Organizing principles for dense packings of nonspherical hard particles: Not all shapes are created equal

Salvatore Torquato and Yang Jiao

Phys. Rev. E **86**, 011102 — Published 5 July 2012

DOI: 10.1103/PhysRevE.86.011102

Organizing Principles for Dense Packings of Nonspherical Hard Particles: Not All Shapes Are Created Equal

Salvatore Torquato*

Department of Chemistry, Department of Physics,

Princeton Center for Theoretical Science,

Program of Applied and Computational Mathematics,

Princeton Institute of the Science and Technology of Materials,

Princeton University, Princeton, New Jersey 08544, USA

Yang Jiao†

Princeton Institute of the Science and Technology of Materials,

Princeton University, Princeton, New Jersey 08544, USA

Abstract

We have recently devised organizing principles to obtain maximally dense packings of the Platonic and Archimedean solids, and certain smoothly-shaped convex nonspherical particles [Torquato and Jiao, Phys. Rev. E **81**, 041310 (2010)]. Here we generalize them in order to guide one to ascertain the densest packings of other convex nonspherical particles as well as *concave* shapes. Our generalized organizing principles are explicitly stated as four distinct propositions. We apply and test all of these organizing principles to the most comprehensive set of both convex and concave particle shapes to date, including Catalan solids, prisms, antiprisms, cylinders, dimers of spheres and various concave polyhedra. We demonstrate that all of the densest known packings associated with this wide spectrum of nonspherical particles are consistent with our propositions. Among other applications, our general organizing principles enable us to construct analytically the densest known packings of certain convex nonspherical particles, including spherocylinders, "lens-shaped" particles, square pyramids and rhombic pyramids. Moreover, we show how to apply these principles to infer the high-density equilibrium crystalline phases of hard convex and concave particles. We also discuss the unique packing attributes of maximally random jammed packings of nonspherical particles.

PACS numbers: 61.50.Ah, 05.20.Jj

*Electronic address: torquato@princeton.edu

†Electronic address: yjiao@princeton.edu

I. INTRODUCTION

Dense packings of hard particles have served as useful models to understand the structure of low-temperature states of matter, such as liquids, glasses, and crystals [1–3], granular media [4], heterogeneous materials [5], and biological systems (e.g., tissue structure, cell membranes, and phyllotaxis) [6–9]. Much of what we know about dense packings concerns particles of spherical shape [9–14], and hence it is useful to summarize key aspects of the *geometric-structure* classification of sphere packings [9] in order to place our results for dense packings of nonspherical particles in their proper context.

The geometric-structure classification naturally emphasizes that there is a great diversity in the types of attainable jammed sphere packings with varying magnitudes of overall order (characterized by scalar order metric ψ that lies in the interval $[0, 1]$), packing fraction ϕ, and other intensive parameters (e.g, mean contact number) [9, 15, 16]. The notions of "order maps" [15] in combination with mathematically precise "jamming categories" [17] enable one to view and characterize well-known packing states, such as the densest sphere packing (Kepler's conjecture) [12] and maximally random jammed (MRJ) packings as extremal states in the order map for a given jamming category [9]. Indeed, this picture encompasses not only these special jammed states, but an uncountably infinite number of other packings, some of which have only recently been identified as physically significant, e.g., the jamming-threshold states (least dense jammed packings) [18] as well as extremal states between these and the MRJ point [16]. Figure 1 shows a schematic order map for frictionless spheres in the ϕ-ψ plane [19] based on our latest knowledge [9, 16].

In recent years, scientific attention has broadened from the study of dense packings of spheres (the simplest shape that does not tile Euclidean space) [12] to dense packings of disordered [20–32] and ordered [33–54] nonspherical particles. The focus of the present paper is on the densest packings of *congruent* nonspherical particles, both convex and concave shapes. We will show that both the symmetry and local principal curvatures of the particle surface play a crucial role in how the rotational degrees of freedom couple with the translational degrees of freedom to determine the maximal density configurations. Thus, different particle shapes will possess maximal density configurations with generally different packing characteristics. We have recently devised organizing principles (in the form of conjectures) to obtain maximally dense packings of a certain class of convex nonspherical hard particles

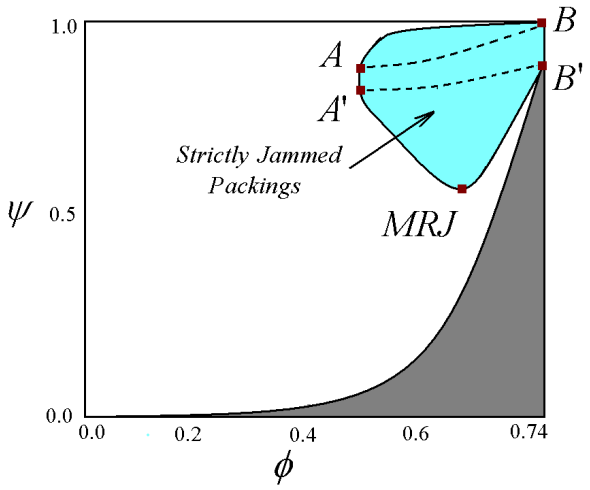

FIG. 1: (Color online) Schematic order map in the density-order ϕ-ψ plane for *strictly* jammed (mechanically stable) packings [17] of frictionless identical spheres in three dimensions (adapted from Ref. [9]). White and blue (or light gray in print version) regions contain the attainable packings, blue regions (or light gray in print version) represent the jammed subspaces, and the dark gray region contains no packings. The locus of points A-A' correspond to the lowest-density jammed packings (thought to be "tunneled crystals" with contact number per particle of exactly 7 [18]). The locus of points B-B' correspond to the densest jammed packings with contact number per particle of exactly 12. Point MRJ represents degenerate maximally random jammed states with a mean contact number per particle $Z = 6$, i.e., the most disordered states subject to the jamming constraint. Although much less is known about the corresponding order maps for nonspherical particles, our current understanding of some of the extremal points shows that they can be quite distinct from their sphere counterparts, as discussed in Secs. III-V.

[41, 42, 45]. Interestingly, our conjecture for certain centrally symmetric polyhedra have been confirmed experimentally very recently [54]. Here we generalize these organizing principles to other convex particles as well as concave shapes [55]. The principles for concave shapes were implicitly given in Ref. [36, 45] and were explicitly stated (without elaboration) elsewhere [55]. Tunability capability via particle shape provides a means to design novel crystal, liquid and glassy states of matter that are richer than can be achieved with spheres (see Fig. 2). While it is seen that hard spheres exhibit entropically driven disorder-order transitions, metastable disordered states, glassy jammed states, and ordered jammed states with maximal density, the corresponding phase diagram for hard nonspherical particles will

generally be considerably richer in complexity due to the rotational degrees of freedom and smoothness of the particle surface (see Sec. IV for further details).

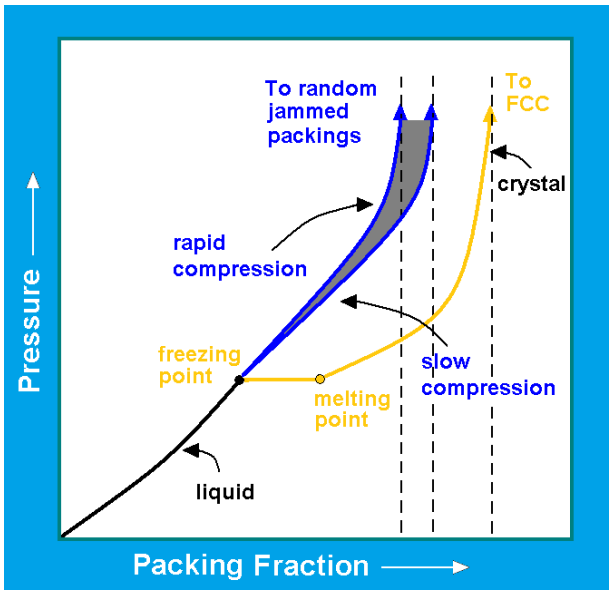

FIG. 2: (Color online) The isothermal phase behavior of three-dimensional hard-sphere model in the pressure-packing fraction plane, adapted from Refs. [5, 9, 56]. Three different isothermal densification paths by which a hard-sphere liquid may jam are shown. An infinitesimal compression rate of the liquid traces out the thermodynamic equilibrium path (shown in yellow or light gray in print version), including a discontinuity resulting from the first-order freezing transition to a crystal branch. Rapid compressions of the liquid while suppressing some degree of local order (curves shown in blue or dark gray in print version) can avoid crystal nucleation (on short time scales) and produce a range of amorphous metastable extensions of the liquid branch (shown in black) that jam only at the their associated terminal densities. The corresponding phase diagrams for nonspherical particles will generally be considerably more complex (see Sec. IV for further details).

Although the focus of the present paper will be the development of organizing principles to obtain dense packings of nonspherical particles in three-dimensional Euclidean space $\mathbb{R}^3$, it is useful to note that such principles have been put forth for two-dimensional convex particles [57–59]. In particular, Fejes-Tóth [57] showed that the densest packing of a centrally symmetric particle in two-dimensional Euclidean space $\mathbb{R}^2$ can be obtained by circumscribing the particle with the minimal centrally symmetric hexagon, which tiles $\mathbb{R}^2$. This leads to

a Bravais-lattice packing (defined in Sec. II) of the centrally symmetric particle under consideration. A key element in his argument is the fact that local optimality is consistent with the global optimality in two dimensions (e.g., a centrally symmetric hexagon can always tessellate the space), which unfortunately generally does not hold in three dimensions. For convex particles in $\mathbb{R}^2$ without central symmetry, Kuperberg and Kuperberg [58] showed that dense packings of a specific particle can be obtained by constructing a *double-lattice* packing of the particle, i.e., a packing composed of a Bravais-lattice packing of the particle itself and a lattice packing of the center-inversion image of the particle. They showed that the maximal-density double-lattice packing of a specific shape can be obtained by minimizing the area of certain parallelogram associated with the packing [60]. We note that the double-lattice packing amounts to a Bravais-lattice packing of a centrally symmetric dimer (i.e., pair) of the original particles.

Generalizing the aforementioned organizing principles to three-dimensional Euclidean space $\mathbb{R}^3$, which is fundamentally different from $\mathbb{R}^2$, is highly nontrivial. In $\mathbb{R}^2$, obtaining the maximally dense packing of a specific particle shape can usually be reduced to a local problem, because the densest local clusters of the particles are frequently consistent with the globally densest packing. However, this principle generally does not apply in $\mathbb{R}^3$, since the densest local packing clusters are usually "geometrically frustrated" [12] and, hence, inconsistent with the globally densest packing. For example, the densest local packing of congruent two-dimensional circles corresponds to an equilateral triangle, which can tessellate $\mathbb{R}^2$. This enables one to easily show that the maximally dense packing of circles in $\mathbb{R}^2$ is the triangular-lattice packing [10]. In $\mathbb{R}^3$, the densest local packing of congruent spheres corresponds to a regular tetrahedron, which cannot completely fill space [40, 61]. This was one reason why it was extremely difficult to prove (taking nearly 400 years) that the maximally dense packings of congruent spheres is achieved by the face-centered-cubic lattice packing (Kepler's conjecture) and its stacking variants [12]. For nonspherical particles in $\mathbb{R}^3$, the situation is even more complex [13] and any proofs establishing the densest packings of nonspherical particles will be considerably more challenging than for spheres. For example, in the densest known packing of regular tetrahedra, the centrally symmetric fundamental packing unit is composed of four tetrahedra [44–46], instead of two as in a double-lattice packing in $\mathbb{R}^2$. It is therefore extremely useful if general organizing principles can be devised to lead one to obtain dense packings of nonspherical particles.

In this paper, we generalize the organizing principles devised for obtaining the maximally dense packings of the Platonic and Archimedean solids and certain smoothly-shaped convex particles (e.g., superballs) to guide one to find the densest packings of other convex nonspherical particles as well as to concave shapes. We explicitly state our generalized organizing principles as four distinct propositions, which are applied and tested to the most comprehensive set of both convex and concave particle shapes to date, including Catalan solids, prisms, antiprisms, cylinders, dimers of spheres and various concave polyhedra. All of the densest known packings associated with the aforementioned large set of nonspherical particles are consistent with our propositions. Moreover, we show that how they can be applied to construct analytically the densest known packings of certain convex nonspherical particles, including spherocylinders and "lens-shaped" particles that are centrally symmetric, as well as square pyramids and rhombic pyramids that lack central symmetry. Although we do not provide rigorous mathematical proofs for our propositions here, we expect that they will either ultimately lead to strict proofs or at least provide crucial guidance in obtaining such proofs for some nonspherical shapes.

Moreover, we show how to apply our organizing principles to infer the high-density equilibrium crystalline phases of hard convex and concave particles. The unique packing attributes of maximally random jammed packings of nonspherical particles are also discussed, which can be used to categorize and characterize MRJ packings according to the particle shapes and symmetries.

The rest of the paper is organized as follows: In Sec. II, we provide preliminaries and basic definitions pertinent to packing problems. In Sec. III, we formulate general organizing principles for dense packings of nonspherical hard particles in the form of four different propositions and test them against the most comprehensive set of the densest known packing constructions of both convex and concave nonspherical particles known to date. In Sec. IV, we present and discuss additional applications of our general organizing principles. Specifically, we construct the densest known packings of centrally symmetric spherocylinders, "lens-shaped" particles, as well as non-centrally symmetric square and rhombic pyramids. We also discuss the expected high-density equilibrium crystal phases of a variety of nonspherical particles as predicted by our propositions. In Sec. V, we make concluding remarks and briefly discuss the unique characteristics of MRJ packings.

II. PRELIMINARIES AND DEFINITIONS

In this section, we provide some basic definitions concerning packings, which closely follow those given in Ref. [9]. A *packing* P is a collection of nonoverlapping solid objects or particles in d-dimensional Euclidean space $\mathbb{R}^d$. Packings can be defined in other spaces (e.g., hyperbolic spaces and compact spaces, such as the surface of a d-dimensional sphere), but our primary focus in this review is $\mathbb{R}^d$. A *saturated* packing is one in which there is no space available to add another particle of the same kind to the packing. A *uniform* packing has a symmetry operation (e.g., a point inversion-symmetric transformation) that takes any particle into another.

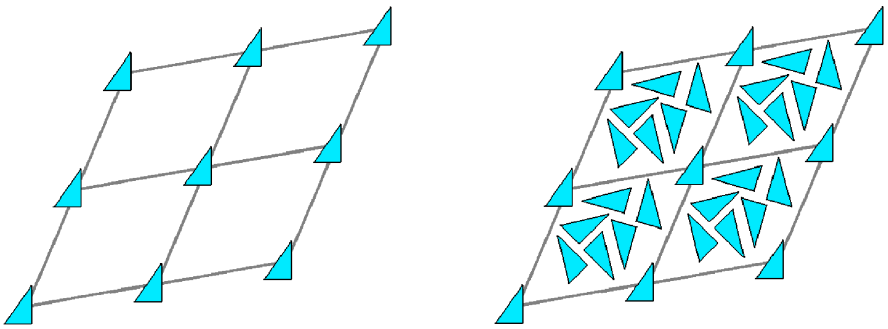

(a) (b)

FIG. 3: (Color online) (a) A portion of a lattice packing of congruent nonspherical particles. Each fundamental cell (depicted as a rhombus here) has exactly one particle centroid. Each particle in the packing must have the same orientation. (b) A portion of a periodic non-lattice packing of congruent nonspherical particles. The fundamental cell contains multiple nonspherical particles with arbitrary positions and orientations within the cell subject to the nonoverlap constraint.

A *lattice* Λ in $\mathbb{R}^d$ is a subgroup consisting of the integer linear combinations of vectors that constitute a basis for $\mathbb{R}^d$. In the physical sciences and engineering, this is referred to as a *Bravais* lattice. Unless otherwise stated, the term "lattice" will refer here to a Bravais lattice only. A *lattice packing* P_L is one in which the centroids of the nonoverlapping identical particles are located at the points of Λ, and all particles have a common orientation. The set of lattice packings is a subset of all possible packings in $\mathbb{R}^d$. In a lattice packing, the space $\mathbb{R}^d$ can be geometrically divided into identical regions F called *fundamental cells*, each of which contains the centroid of just one particle. Thus, the density of a lattice packing is

given by

$$\phi = \frac{v_1}{\mathrm{Vol}(F)}, \tag{1}$$

where v_1 is the volume of a single d-dimensional particle and $\mathrm{Vol}(F)$ is the d-dimensional volume of the fundamental cell. For example, the volume $v_1(R)$ of a d-dimensional spherical particle of radius R is given explicitly by

$$v_1(R) = \frac{\pi^{d/2} R^d}{\Gamma(1 + d/2)}, \tag{2}$$

where $\Gamma(x)$ is the Euler gamma function. Figure 3(a) depicts lattice packings of congruent spheres and congruent nonspherical particles.

A more general notion than a lattice packing is a periodic packing. A *periodic* packing of congruent particles is obtained by placing a fixed configuration of N particles (where $N \geq 1$) with *arbitrary nonoverlapping orientations* in one fundamental cell of a lattice Λ, which is then periodically replicated without overlaps. Thus, the packing is still periodic under translations by Λ, but the N particles can occur anywhere in the chosen fundamental cell subject to the overall nonoverlap condition. The packing density of a periodic packing is given by

$$\phi = \frac{N v_1}{\mathrm{Vol}(F)} = \rho v_1, \tag{3}$$

where $\rho = N/\mathrm{Vol}(F)$ is the number density, i.e., the number of particles per unit volume. Figure 3(b) depicts a periodic non-lattice packing of congruent spheres and congruent nonspherical particles. Note that the particle orientations within a fundamental cell in the latter case are generally not identical to one another.

We will see subsequently that certain characteristics of particle shape, e.g., whether it possesses central symmetry and equivalent principal axes, play a fundamental role in determining its dense packing configurations. A d-dimensional particle is *centrally symmetric* if it has a center C that bisects every chord through C connecting any two boundary points of the particle, i.e., the center is a point of inversion symmetry. Examples of centrally symmetric particles in $\mathbb{R}^d$ include spheres, ellipsoids and superballs (see Ref. [9] for definitions of these shapes). A triangle and tetrahedron are examples of non-centrally symmetric two- and three-dimensional particles, respectively. Figure 4 depicts examples of centrally and non-centrally symmetric two-dimensional particles. A d-dimensional centrally symmetric particle for $d \geq 2$ is said to possess d equivalent principal (orthogonal) axes (directions)

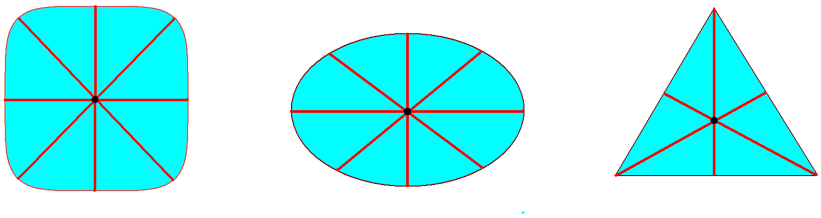

(a) (b) (c)

FIG. 4: (Color online) (a) A "superdisk" is centrally symmetric and possesses two equivalent principal axes. (b) An ellipse is centrally symmetric but does not possess two equivalent principal axes. (c) A triangle is not centrally symmetric.

associated with the moment of inertia tensor if those directions are two-fold rotational symmetry axes such that the d chords along those directions and connecting the respective pair of particle-boundary points are equal. (For $d = 2$, the two-fold (out-of-plane) rotation along an orthogonal axis brings the shape to itself, implying the rotation axis is a "mirror image" axis.) Whereas a d-dimensional superball has d equivalent directions, a d-dimensional ellipsoid generally does not (see Fig. 4).

III. GENERAL ORGANIZING PRINCIPLES

We have formulated several organizing principles in the form of three conjectures for convex polyhedra as well as other nonspherical convex shapes [41, 42, 45, 49]. In this section, we generalize them in order to guide one to ascertain the densest packings of other convex nonspherical particles as well as *concave* shapes based on the characteristics of the particle shape (e.g., symmetry, principal axes and local principal curvature). The generalized organizing principles are explicitly stated as four distinct propositions. We apply and test all of these organizing principles to the most comprehensive set of both convex and concave particle shapes to date, including Catalan solids, prisms, antiprisms, cylinders, dimers of spheres and various concave polyhedra. We demonstrate that all of the densest known packings associated with this wide spectrum of nonspherical particles are consistent with our propositions. In Sec. IV, we will apply our propositions to construct analytically the densest known packings of other nonspherical particles, including spherocylinders and "lens-

shaped" particles that are centrally symmetric, as well as square and rhombic pyramids that lack central symmetry. We also apply the organizing principles to infer the high-density equilibrium crystalline phases of hard convex and concave particles in Sec. IV.

A. Organizing Principles for Convex Particles

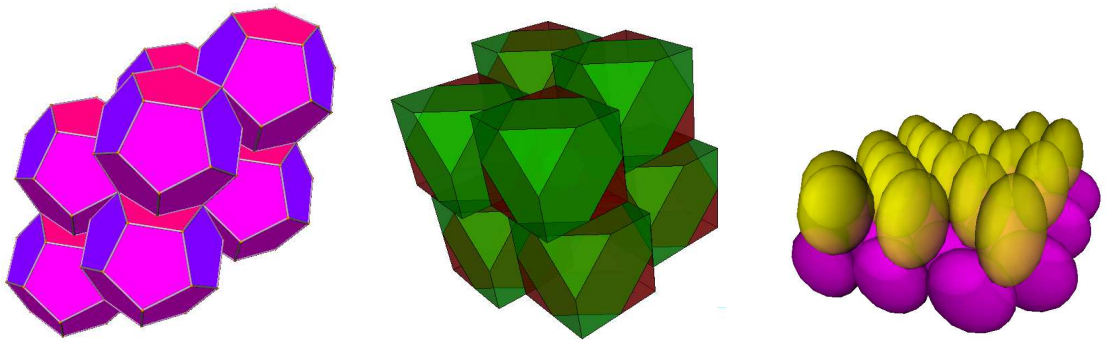

(a) (b) (c)

FIG. 5: (Color online) Dense packings of nonspherical particles. (a) A portion of the densest lattice packing of dodecahedra, which possess central symmetry. (b) A portion of the densest known packing of truncated tetrahedra without central symmetry. In the packing, the truncated tetrahedra form centrally symmetric dimers and the dimers pack on a lattice. (c) A portion of the densest known packing of oblate ellipsoids, which contains two ellipsoids perpendicular to one another in the fundamental cell.

For the centrally symmetric Platonic and Archimedean solids, our simulations and theoretical analysis lead us to the following conjecture [41, 42]:

Conjecture 1: *The densest packings of the centrally symmetric Platonic and Archimedean solids are given by their corresponding optimal Bravais lattice packings.*

Remarks: The centrally symmetric Platonic and Archimedean solids are polyhedra with three equivalent principal axes. For packings of polyhedra, face-to-face contacts are favored over other types of contacts (e.g., face-to-edge, face-to-vertex, edge-to-edge etc.), since the former allow the particle centroids to get closer to one another and thus, to achieve higher packing densities. For centrally symmetric polyhedra, aligning the particles (i.e., all in the same orientation) enable a larger number of face-to-face contacts. For example, a particle

with F faces, possesses $F/2$ families of axes that go through the centroid of the particle and intersect the centrally-symmetric face pairs such that the particles (in the same orientation) with their centroids arranged on these axes can form face-to-face contacts. The requirement that the particles have the same orientation is globally consistent with a (Bravais) lattice packing. Indeed, in the optimal lattice packings of the centrally symmetric Platonic and Archimedean solids, each particle has the maximum number of face-to-face contacts that could possibly be obtained without violating the nonoverlapping conditions. It is highly unlikely that such particles possessing three equivalent principal axes and aligned in the same direction could form a more complicated non-lattice periodic packings with densities that are larger than the optimal lattice packings.

Conjecture 1 is the analog of Kepler's sphere conjecture for the centrally symmetric Platonic and Archimedean solids. In this sense, such solids behave similarly to spheres in that their densest packings are lattice arrangements and (except for the cube) are geometrically frustrated like spheres. This conjecture was strongly supported by our original simulations of the Platonic solids [41, 42], which used multiple-particle configurations in the fundamental cell and only produce the optimal lattice packings. More recently, dense packings of other polyhedra have been numerically investigated, including the Archimedean solids [49, 52], Catalan solids [52], Johnson solids [52], prisms and antiprisms [52], and a family of truncated tetrahedra [50]. Among this large set of polyhedra, it has been found that for centrally symmetric shapes, numerical simulations with multiple particles in the fundamental cell always converge to dense lattice packings, which possess higher densities than all other periodic packing configurations. These finding support Conjecture 1. Certain characteristics of densest known packings of a subset of the aforementioned polyhedra are provided in Table I and Table II, including the type of the packing structure (lattice or periodic) and the packing density (both numerical value and analytical value if known).

In addition to the strong numerical evidence for Conjecture 1, we have derived a simple *analytical* upper bound on the maximal density ϕ_{max} of a packing of congruent nonspherical particles of volume v_p in any Euclidean space dimension d in terms of the maximal density of a d-dimensional packing of congruent spheres of volume v_s, which is the volume of the largest sphere than can be inscribed in the nonspherical particle. Here, for simplicity, we state that upper bound for three-dimensions:

TABLE I: Characteristics of dense packings of Platonic and Archimedean solids, including whether the particle possesses central symmetry, whether the packing is a Bravais lattice packing, the number of basis particles in the fundamental cell if the packing is a non-Bravais-lattice periodic packing, the numerically obtained packing density ϕ^* [41, 42, 52], the analytically obtained density ϕ_{max} [39], and the upper bound on the density ϕ^U_{max} [41, 42].

Polyhedron	Cen. Sym.	Structure	ϕ^*	ϕ_{max}	ϕ^U_{max}
Tetrahedron	No	Periodic, 4-particle basis	0.8560	0.856347	1
Icosahedron	Yes	Bravais Lattice	0.8361	0.836357	0.893417
Dodecahedron	Yes	Bravais Lattice	0.9042	0.904508	0.981162
Octahedron	Yes	Bravais Lattice	0.9471	0.947368	1
Cube	Yes	Bravais Lattice	0.9999	1	1
Truncated Tetrahedron	No	Periodic, 2-particle basis	0.9885	0.995192	1
Truncated Icosahedron	Yes	Bravais Lattice	0.7849	0.784987	0.838563
Snub Cube	No	Bravais Lattice	0.7876	0.787699	0.934921
Snub Dodecahedron	No	Bravais Lattice	0.7874	0.788640	0.855474
Rhombicicosidodecahedron	Yes	Bravais Lattice	0.8047	0.804708	0.835964
Truncated Icosidodecahedron	Yes	Bravais Lattice	0.8269	0.827213	0.897316
Truncated Cuboctahedron	Yes	Bravais Lattice	0.8489	0.849373	0.875805
Icosidodecahedron	Yes	Bravais Lattice	0.8644	0.864720	0.938002
Rhombicuboctahedron	Yes	Bravais Lattice	0.8758	0.875805	1
Truncated Dodecahedron	Yes	Bravais Lattice	0.8976	0.897787	0.973871
Cuboctahedron	Yes	Bravais Lattice	0.9182	0.918367	1
Truncated Cube	Yes	Bravais Lattice	0.9722	0.973747	1
Truncated Octahedron	Yes	Bravais Lattice	0.9999	1	1

Lemma: *The maximal density of a packing of congruent nonspherical particles is bounded from above according to the following bound [41, 42]*

$$\phi_{max} \leq min\left[\frac{v_p}{v_s}\frac{\pi}{\sqrt{18}},\ 1\right], \tag{4}$$

where $min[x, y]$ *denotes the minimum of* x *and* y.

The upper bound values for a subset of the aforementioned polyhedra are give in Table I

TABLE II: Characteristics of dense packings of Catalan solids and certain prisms, including whether the particle possesses central symmetry, whether the packing is a Bravais lattice packing, the number of basis particles in the fundamental cell if the packing is a non-Bravais-lattice periodic packing [52], the numerically obtained packing density ϕ^* [52], and the upper bound on the density ϕ^U_{max} [52].

Polyhedron	Cen. Sym.	Structure	ϕ^*	ϕ^U_{max}
Pentagonal Hexecontrahedron	No	Bravais Lattice	0.741075	0.782834
Pentagonal Icositetrahedron	No	Periodic, 2-particle basis	0.743639	0.848563
Pentakis Dodecahedron	Yes	Bravais Lattice	0.757552	0.787991
Disdyakis Triacontrahedron	Yes	Bravais Lattice	0.765496	0.773134
Deltoidal Hexecontrahedron	Yes	Bravais Lattice	0.77155	0.782871
Disdyakis Dodecahedon	Yes	Bravais Lattice	0.793288	0.813656
Deltoidal Icositetrahedron	Yes	Bravais Lattice	0.796934	0.851348
Triakis Tetrahedron	No	Periodic, 4-particle basis	0.798868	1
Rhombic Triacontrahedron	Yes	Bravais Lattice	0.801741	0.834626
Triakis Icosahedron	Yes	Bravais Lattice	0.804796	0.818047
Tetrakis Hexahedron	Yes	Bravais Lattice	0.814019	0.878410
Small Triakis Octahedron	Yes	Bravais Lattice	0.876016	0.937283
Rhombic Dodecahedron	Yes	Bravais Lattice	1	1
Heptaprism	No	Periodic, 2-particle basis	0.896	1
Pentaprism	No	Periodic, 2-particle basis	0.921	1

and Table II. As noted in Ref. [42], the upper bound (4) is generally not sharp, i.e., it generally can not be realized, except for certain space-filling shapes. Therefore, a small difference between the actual packing density and the corresponding upper bound value strongly suggests the optimality of the packing. It can be seen from Tables I and II that the difference is indeed small for centrally symmetric polyhedra with equivalent principal axes. Together with the numerical evidence, this leads us to the following more general proposition:

Proposition 1: *Dense packings of centrally symmetric convex, congruent polyhedra with*

three equivalent axes are given by their corresponding densest lattice packings, providing a tight density lower bound that may be optimal.

Remarks: This proposition is the three-dimensional analog of the Fejes-Tóth theorem for two-dimensional centrally symmetric shapes [57]. Note that whenever Proposition 1 leads to an optimal packing, one can immediately obtain an upper bound on ϕ_{max} that improves upon inequality (4). Namely, for a general nonspherical particle of volume v_p, instead of inscribing into the particle the largest possible sphere, one can inscribe the largest possible polyhedron with known maximal packing density, i.e.,

$$\phi_{max} \leq \min \left[\frac{v_p}{v_0} \phi^0_{max},\ 1 \right], \tag{5}$$

where v_0 denotes the volume of the largest centrally symmetric convex particle with three equivalent axes that can be inscribed in the nonspherical particle of interest and ϕ^0_{max} is its associated maximal density. In the case that ϕ^0_{max} can be proven to be optimal, (5) is a rigorous upper bound. Otherwise, it provides an estimate of ϕ_{max}.

As an application of inequality (5), consider inscribing a truncated dodecahedron into a dodecahedron. Assuming that $\phi^0_{max} = 0.897787$ for the optimal truncated dodecahedron packing leads to an estimate of $\phi^* = 0.904508$ for the densest dodecahedron packing, which is identical to the actual value $\phi_{max} = 0.904508$ for the densest *lattice* packing of dodecahedra. In general, the inscribed polyhedron should be chosen carefully in order to get a nontrivial upper bound. In the case that the optimality of the packing of the inscribed polyhedron can be proven, this could lead to tight upper bound on ϕ_{max} for nonspherical particles improved over the simple sphere bound (4).

Note that the space-filling polyhedra in the aforementioned three families of shapes, i.e., the cube, the truncated octahedron (one of the Archimedean solids) and the rhombic dodecahedron (dual of the Catalan cuboctahedron) are respectively the Voronoi cells associated with the simple cubic, body-centered cubic and face-centered cubic lattices [5]. The densest packings of cubes can be achieved by an uncountably infinite number of non-lattice packings corresponding to sliding layers or chains of cubes in their simple cubic lattice packing [42]. By contrast, we note here that the densest Bravais-lattice packings of the truncated octahedron and the rhombic dodecahedron are the unique densest packings of the two shapes. In contrast to the densest lattice packing of cubes, in the densest lattice packings of the truncated octahedron and the rhombic dodecahedron, no chains or layers of particles can

slide relative to one another. Thus, there are no collective motions within the densest packings [48] of the truncated octahedron and the rhombic dodecahedron that can lead to other non-lattice packings of the two shapes that can completely fill space.

We also note that both simulations [37, 38] and analytical constructions [37] suggest that the optimal packings of superballs, a rich family of smoothly-shaped centrally symmetric particles with both octahedral and cubic symmetry including a three-dimensional cross limit, are their densest Bravais lattice packings. This suggests that Conjecture 1 can be generalized not only to polyhedral particles but also to certain smoothly-shaped particles. A major distinction between a smoothly-shaped particle and a polyhedron is that the surface of the former possesses non-trivial local principal curvatures, which are either zero or infinity. We note that a complete understanding of the role of curvature in determining dense packing configurations is currently lacking, although it has been shown that curvature is crucial for stabilized disordered packings of nonspherical particles [20, 22].

For convex polyhedral particles that lack central symmetry, we have made the following conjecture concerning their densest packing configurations [41, 42]:

Conjecture 2: *The densest packing of any convex, congruent polyhedron without central symmetry generally is not a Bravais lattice packing, i.e., set of such polyhedra whose optimal packing is not a Bravais lattice is overwhelmingly larger than the set whose optimal packing is a Bravais lattice.*

Remarks: In other words, Conjecture 2 states that the set of non-centrally symmetric polyhedra whose optimal packing is not a lattice is overwhelmingly larger than the set whose optimal packing is a lattice. As shown in Table I and Table II, the fact that the regular tetrahedron and truncated tetrahedron lack central symmetry and that dense packings of such objects favor face-to-face contacts immediately eliminates the possibility that lattice packings (in which particles must have the same orientations and thus, have face-to-vertex contacts) are optimal. Similarly, it is very plausible that dense packings of most convex, congruent polyhedra without central symmetry are facilitated by face-to-face contacts by exploring their rotational degrees of freedom and hence the optimal packings are generally not lattice packings. This reasoning immediately leads us to the following more general proposition concerning dense packings of polyhedra without central symmetry:

Proposition 2: *Dense packings of convex, congruent polyhedra without central symmetry*

are composed of centrally symmetric compound units of the polyhedra with the inversion-symmetric points lying on the densest lattice associated with the compound units, providing a tight density lower bound that may be optimal.

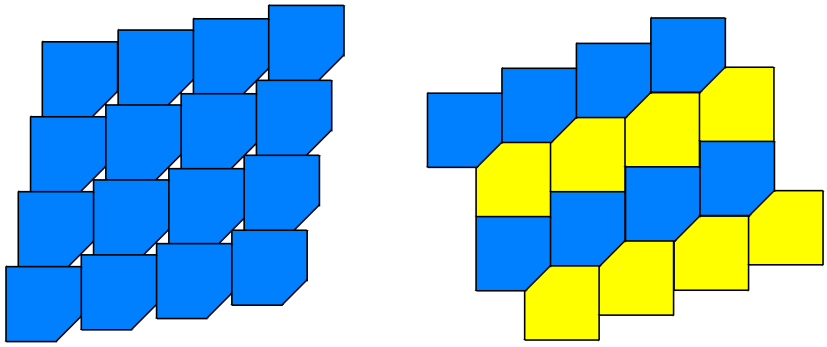

(a) (b)

FIG. 6: (Color online) Portions of two packing configurations of pentagons obtained by cutting off a corner (isosceles triangle with a right angle) of a square (adapted from Ref. [42]). (a) The optimal lattice packing and (b) a two-particle basis periodic packing that tiles the plane. Let side length of the square be 1 and the lengths of the equal sides of the isosceles triangle be $\beta \in (0, 1)$. The lattice vectors of the optimal lattice packing are $\mathbf{e}_1^L = \mathbf{i} - \frac{\beta}{2}\mathbf{j}$, $\mathbf{e}_2^L = (1 - \frac{\beta}{2})\mathbf{i} + (1 - \beta)\mathbf{j}$ and the lattice vectors of the periodic packing are $\mathbf{e}_1^P = \mathbf{i} + \beta\mathbf{j}$, $\mathbf{e}_2^P = (1 - \beta)\mathbf{i} + (2 - \beta)\mathbf{j}$ with one particle at origin and the other at $\mathbf{b}_1 = (1 - \beta)\mathbf{i} + (1 - \beta)\mathbf{j}$, where $\mathbf{i}, \mathbf{j}$ are the unit vectors along the two orthogonal coordinate directions, coinciding with two orthogonal sides of the square. The density (covering fraction) of the optimal lattice packing is $\phi_{max}^L = (1 - \frac{\beta^2}{2})/(1 - \frac{\beta^2}{4})$ and the density of the periodic packing is $\phi_{max}^P = 1$. It can be seen that for all $0 < \beta < 1$, ϕ_{max}^L is always smaller than ϕ_{max}^P.

Remarks: Application of this proposition can be very well illustrated by the "truncated square" example originally given in Ref. [42]. We note that although this specific example involves polygons in two dimensions, the general idea that lacking central symmetry enables the full exploration of the rotational degrees of freedom associated with a nonspherical particle in obtaining the densest packing also applies in three dimensions. Specifically, consider a square with one missing corner, i.e., an isosceles triangle with a right angle (see Fig. 6). At first glance, one might surmise that if the missing piece is sufficiently small, a

lattice packing which is close to the original square lattice packing should still be optimal (see Fig. 6a), since lattice packings are optimal for squares. However, no matter how small the missing piece may be, a periodic packing in which the fundamental cell contains two truncated squares can be constructed that tile the plane (see Fig. 6b). This is done by taking advantage of the asymmetry of the particle to maximize possible face-to-face contacts. Thus, we see from this counterintuitive example that if the particle does not possess central symmetry, it is possible to exploit its rotational degrees of freedom to yield a periodic packing with a complex basis that are generally denser than the optimal lattice packing. We also note that Proposition 2 can be considered as the three-dimensional analog of Kuperberg-Kuperberg double-lattice packing constructions for two-dimensional convex shapes lacking central symmetry [58].

On the other hand, there are special cases where the lattice will be optimal for particles lacking central symmetry. One such example in three dimensions is the rhombic dodecahedron that has one corner clipped [12, 42]. Another one involves the Archimedean snub cube and snub dodecahedron, which are chiral shapes (and therefore, non-centrally symmetric) [52]. However, these chiral polyhedra still possess pairs of parallel faces as a centrally symmetric particle, which allows the maximum number of face-to-face contact when aligned. Nonetheless, these special cases are overwhelmed in number by the set of those whose optimal packings are not lattices. We also note that if Conjecture 2 is valid, it also applies to nonspherical particles derived by smoothing the vertices, edges and faces of polyhedra provided that the local curvature at face-to-face contacts is sufficiently small.

Finally, we note that for certain centrally symmetric particles that do not possess three equivalent principal axes (e.g., ellipsoids [35]), the rotational degrees of freedom of the particle can be explored, resulting in dense non-Bravais-lattice packings. This observation had led us to the following conjecture [45]:

Conjecture 3: *The densest packings of congruent, centrally symmetric particles that do not possesses three equivalent principle axes (e.g., ellipsoids) can be non-Bravais lattices.*

Remarks: For a general smoothly-shaped particle, the local principal curvature of the particle surface plays an important role in determining their densest packing configurations. This is to contrast polyhedral particles with flat faces, whose dense packings are determined solely by maximizing face-to-face contacts. For ellipsoids, the local principal curvature at

any point on the surface possesses non-trivial values. Bezdek and Kuperberg were the first to show that the densest packings of very elongated ellipsoids cannot be Bravais lattice packings [33]. In particular, by inserting very elongated ellipsoids into cylindrical void channels passing through the "ellipsoidal" analogs of the face-centered-cubic sphere packing (affinely deformed face-centered-cubic packings of spheres), Bezdek and Kuperberg constructed congruent ellipsoid packings whose density exceeds $\pi/\sqrt{18}$ and approaches 0.7459 in the limit of infinitely thin prolate spheroids (i.e., the "needle" limit). Later, Wills [34] showed that similar constructions can be obtained by inserting needle-like ellipsoids into cylindrical void channels passing through an affinely deformed hexagonal-close-packed lattice of spheres, leading to an improved density of 0.7585. More recently, Donev et al. [35] found a family of unusually dense non-Bravais-lattice packings of ellipsoids with *arbitrary* aspect ratio. The packings in this family have two ellipsoids per fundamental cell, rotated by $\pi/2$ relative to one another, and possess packing densities as high as 0.7707 when the maximal aspect ratio is larger than $\sqrt{3}$, which is close to the sphere shape.

Finally, we note that non-Bravais lattice packings of elliptical cylinders (i.e., cylinders with an elliptical basal face) that are denser than the corresponding optimal lattice packings have been constructed [33]. This result supports our Conjecture 3.

B. Organizing Principles for Concave Particles

As pointed in the previous section, dense packings of convex polyhedra favor a large number of face-to-face contacts between neighboring particles, which can be achieved by either a lattice packing or a periodic one depending on the particle characteristics. It should not go unnoticed that our arguments leading to our conjectures and propositions thus far do not rely on the convexity of the particle shape and hence does not seem to be a strongly limiting condition. Indeed, in this section, we generalize the propositions to obtain appropriate propositions for concave polyhedron particles.

We state the generalization of Proposition 1 for concave particles as a proposition:

Proposition 3: *Dense packings of centrally symmetric concave, congruent polyhedra are given by their corresponding densest lattice packings, providing a tight density lower bound that may be optimal.*

Similarly, the generalization of Proposition 2 is given by the following proposition:

Proposition 4: *Dense packings of concave, congruent polyhedra without central symmetry are composed of centrally symmetric compound units of the polyhedra with the inversion-symmetric points lying on the densest lattice associated with the compound units, providing a tight density lower bound that may be optimal.*

Remarks: Due to the translational symmetry of a periodic packing, the centrally symmetric compound unit can be located anywhere within the fundamental cell. In practice, it is usually more convenient to place the centroid of an original polyhedron on the lattice points than to place the inversion center of the compound unit on them. Note also that for concave shapes, even the densest packing could possess a density that is much smaller than unity. Therefore, the term "dense" in the above two propositions means that the packing possesses a relatively high density compared to that of other packings of the same concave shape.

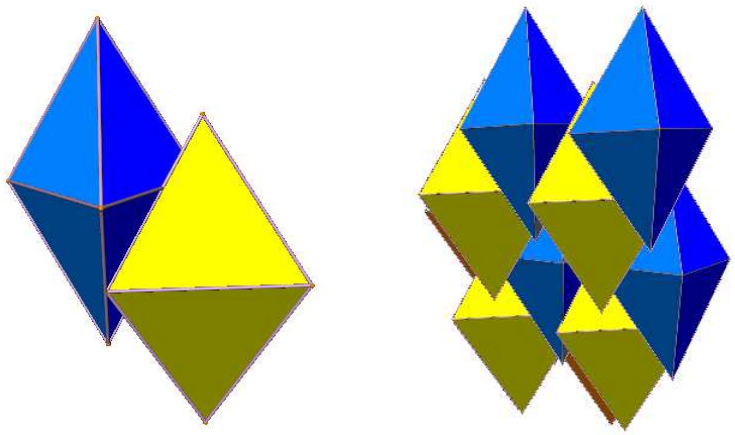

(a) (b)

FIG. 7: (Color online) (a) A centrally symmetric concave compound unit of tetrahedra, which is composed of two contacting dimers of tetrahedra. (b) A portion of the densest known packing of tetrahedra, which is a lattice packing of the centrally symmetric compound unit.

Our new propositions for concave shapes are in fact motivated by our investigation of the densest known packings of regular tetrahedra, which are periodic packings with four particles in the fundamental cell [44–46]. It was already noted in Ref. [45] that the 4-particle compound object in the fundamental cell composed of two contacting dimers (i.e., two tetrahedra forming perfectly face-to-face contact) possesses center inversion symmetry

and thus, it can be viewed as a centrally symmetric *concave polyhedron*, see Fig. 7. Hence, the densest known packings of tetrahedra are in fact Bravais-lattice packings of such *concave compound polyhedra*. Based on the same arguments leading to Propositions 1 and 2 [41, 42], it is not surprising that dense Bravais-lattice packings of the centrally symmetric compound polyhedra have a high density, since there are a large number of face-to-face contacts, which are made possible due to the central symmetry of the compound polyhedron and bring the centroids of the objects closer to each other, despite of the concave nature of the compound polyhedron.

TABLE III: Characteristics of dense packings of certain concave polyhedral particles, including whether the particle possesses central symmetry, whether the densest known packing is a Bravais lattice packing, the number of basis particles in the fundamental cell if the packing is a non-Bravais-lattice periodic packing [52], the numerically obtained density ϕ^*_{lat} for the lattice packing [52], the highest numerically obtained density ϕ^* [52], and the upper bound on the density ϕ^U_{max} [52].

Polyhedron	Cen. Sym.	Structure	ϕ^*_{lat}	ϕ^*	ϕ^U_{max}
Császár Polyhedron	No	Periodic, 4-particle basis	0.381	0.631	1
Szilassi Polyhedron	No	Periodic, 2-particle basis	0.331	0.519	1
Echidnahedron	Yes	Bravais Lattice	0.294	0.294	1
Escher's Solid	Yes	Bravais Lattice	0.947	0.947	1
Great Rhombic Triacontahedron	Yes	Bravais Lattice	0.557	0.557	1
Jessen's Orthogonal Icosahedron	Yes	Bravais Lattice	0.749	0.749	1
Rhombic Dodecahedron Stellation II	Yes	Bravais Lattice	0.599	0.599	1
Great Stellated Dodecahedron	Yes	Periodic, 2-particle basis	0.857	0.889	1
Rhombic Hexecontahedron	Yes	Periodic, 2-particle basis	0.529	0.556	1
Small Triambic Icosahedron	Yes	Periodic, 2-particle basis	0.688	0.695	0.977
Nanostar	Yes	Bravais Lattice	0.686	0.686	1
Octapod	Yes	Bravais Lattice	0.310	0.310	1
Tetrapod	No	Periodic, 2-particle basis	0.591	0.592	1

Very recently, de Graaf, van Roij and Dijkstra [52] numerically generated the densest known packings of a variety of concave particles, including certain well-known concave polyhedra and approximations of real concave nanoparticles. In Table III, we provide certain

packing characteristics of a subset of the concave polyhedra studied by these authors.

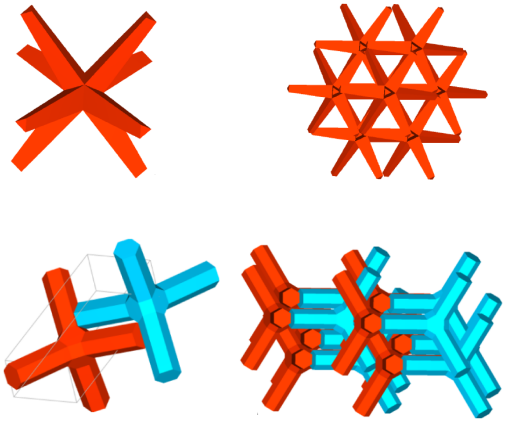

FIG. 8: (Color online) Densest known packings of concave particles (adapted from Ref. [52], image courtesy of de Graaf, van Roij and Dijkstra). Upper panel: a centrally symmetric octapod (left) and the corresponding densest known packing (right), which is a lattice packing of octapods. Lower panel: a dimer of non-centrally symmetric tetrapods (left) and the corresponding densest known packing (right), which is periodic packing with two tetrapods in the fundamental cell.

Despite the concavity of these particles, it can be clearly seen from Table III that for centrally symmetric shapes, the densest lattice packings either correspond to the obtained densest packings or provide a very tight lower bound on the densest packings, which are consistent with our propositions. In fact, for the three centrally symmetric solids (great stellated dodecahedron, rhombic hexecontahedron, and small triambic icosahedron) whose densest packings obtained are not lattice packings, the difference in the packing density between the obtained lattice packing and densest packing is very small (i.e., less than 3%). Given the complexity of the particle shapes involved, it could be possible that the numerical method was not able to obtain the corresponding optimal lattice packings. On the other hand, for shapes lacking central symmetry, the densest packings always correspond to lattice packings of the centrally symmetric compound objects composed of the original polyhedra, and thus, are periodic packings of the original polyhedra. We note that due to the large asphericity (i.e., the ratio of circumsphere radius over insphere radius of the particle [42]) associated with concave shapes, the upper bound (4) for many concave polyhedra gives trivial value of unity, which is usually much larger than the highest packing densities obtained. Nonetheless, the robustness of the numerical procedure for generating the dense packings

of concave particles has been verified by virtually producing the densest known packings of the Platonic and Archimedean solids, among other shapes [52]. Therefore, it is reasonable to believe that most of the numerical packings of the concave particles obtained from the computer simulations in Ref. [52] are close to optimal. Nonetheless, all of the densest known packings of the large set of the concave particles shown in Table III are consistent with Propositions 3 and 4.

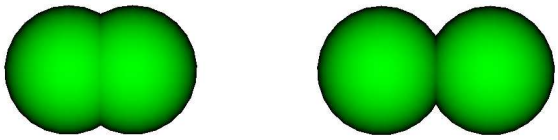

FIG. 9: (Color online) Dimers of spheres of radius R, with sphere center separation L. Left panel: A dimer of spheres with aspect ratio $L/R = 0.85$. Right panel: A dimer of spheres with aspect ratio $L/R = 1.85$, in which the two spheres just touch each other.

Finally, we note that our Propositions 3 and 4 should also apply for certain smoothly-shaped concave particles. For example, consider the family of dimers formed by two spheres in $\mathbb{R}^3$ that can overlap to various degrees (see Fig. 9), whose volume is given by

$$V_0 = \frac{4\pi}{3}R^3\left(1 + \frac{3}{4}\frac{L}{R} - \frac{1}{16}\frac{L^3}{R^3}\right), \tag{6}$$

where R is the radius of the spheres and $L \in [0, 2R]$ is the separation between the sphere centers. This family of dimers of spheres includes the single-sphere case and the two-touching-sphere case as extreme cases. Since such a dimer possesses central symmetry, the densest packing of this shape can be expected to be a lattice packing according to Propositions 3. Indeed, it has been shown that in both $\mathbb{R}^2$ [63] and $\mathbb{R}^3$ [64], the densest known dimer-sphere packings are achieved by certain Bravais lattices.

IV. ADDITIONAL APPLICATIONS OF THE ORGANIZING PRINCIPLES

In this section, we illustrate how the general organizing principles formulated in the previous sections can be applied in practice. Specifically, Propositions 1-4 provide constructable tight lower bounds on dense packings of both centrally symmetric polyhedra and the ones lacking central symmetry. These organizing principles should enable one to construct dense packings of a specific nonspherical shape, which are either optimal or close to optimal. We

demonstrate this capability by finding the densest known packings of centrally symmetric spherocylinders, and "lens-shaped" particles as well as non-centrally symmetric square pyramids and rhombic pyramids. In addition, we show that analytically constructed dense packing configurations as determined by our organizing principles can serve as the starting point to study the equilibrium phase behavior of the corresponding particles at high densities [49, 53, 65–69].

A. Dense packings of spherocylinders

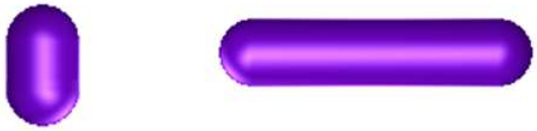

FIG. 10: (Color online) Spherocylinders composed of cylinder with length L, caped at both ends with hemispheres with radius R. Left panel: A spherocylinder with aspect ratio $L/R = 1$. Right panel: A spherocylinder with aspect ratio $L/R = 5$.

Let us now consider the case of a spherocylinder. A spherocylinder consists of an cylinder with length L and radius R capped at both ends by hemispheres with radius R (see Fig. 10), and therefore is a centrally-symmetric convex particle. Its volume is given by

$$V_0 = \pi R^2 L + \frac{4}{3}\pi R^3. \tag{7}$$

At the limit $L = 0$, a spherocylinder reduces to a sphere with radius R.

For spherocylinders with $L > 0$, it appears that the optimal Bravais-lattice packing could be the actual densest packing of the shape. This is because the local principal curvature of the cylindrical surface is zero along the spherocylinder axis, and thus, spherocylinders can have very dense lattice packings by aligning the cylinders along their axes. The density of the optimal Bravais-lattice packing of spherocylinders is given by

$$\phi = \frac{\pi}{\sqrt{12}} \frac{L + \frac{4}{3}R}{L + \frac{2\sqrt{6}}{3}R}, \tag{8}$$

where L is the length of the cylinder and R is the radius of the spherical caps [62]. However, we note that there are a noncountably-infinite number of non-Bravais-lattice packings of

spherocylinders with the same packing densities (8), associated with the infinite number of different stackings of spherocylinder layers similar to the Barlow stackings of the spheres [9]. Thus, the set of dense non-lattice packings of spherocylinders is overwhelmingly larger than that of the lattice packing. We emphasize that the role of the local principal curvature of the particle surface in determining dense packing configurations is far from being completely understood.

B. Dense packings of "lens-shaped" particles

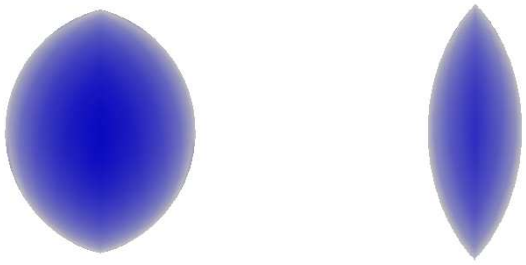

FIG. 11: (Color online) "Lens-shaped" particles corresponding to the intersection regions of two spheres with radius R separated by distance L. Left panel: A lens-shaped particle associated with $L/R = 0.8$. Right panel: A lens-shaped particle associated with $L/R = 1.6$.

Let us also consider dense packings of "lens-shaped" particles, which correspond to the intersection region of two congruent spheres, and therefore is a centrally-symmetric convex particle. In particular, the volume of such a lens-shaped particle is given by

$$V_0 = \frac{4\pi}{3} R^3 \left(1 - \frac{3}{4}\frac{L}{R} + \frac{1}{16}\frac{L^3}{R^3} \right), \tag{9}$$

where R is the radius of the spheres and $L \in [0, 2R)$ is the separation distance between the sphere centers.

Similar to the aforementioned case of spherocylinders, it appears that both the optimal Bravais-lattice packing of such lens-shaped particles, corresponding to the FCC-like stacking of the triangular-lattice layers of the particles, and the noncountably-infinite number of Barlow-like stackings of the layers give the densest known packings, which possess densities given by

$$\phi = \frac{8\pi}{\sqrt{3}} \frac{1 - \frac{3}{4}\frac{L}{R} + \frac{1}{16}\frac{L^3}{R^3}}{(4 - \frac{L^2}{R^2})[(24 + \frac{3L^2}{R^2})^{\frac{1}{2}} - \frac{3L}{R}]}. \tag{10}$$

Note that in the sphere limit (i.e., $L = 0$), one can obtain the optimal sphere-packing density $\phi = \pi/\sqrt{18}$. In the limit of infinitely thin "lenses" ($L \to 2$), one has $\phi = \sqrt{3}\pi/8$. However, we do not exclude the possibility that there exist other Bravais-lattice or non-lattice packings that are denser than our current constructions.

C. Dense packings of pyramids from octahedron packing

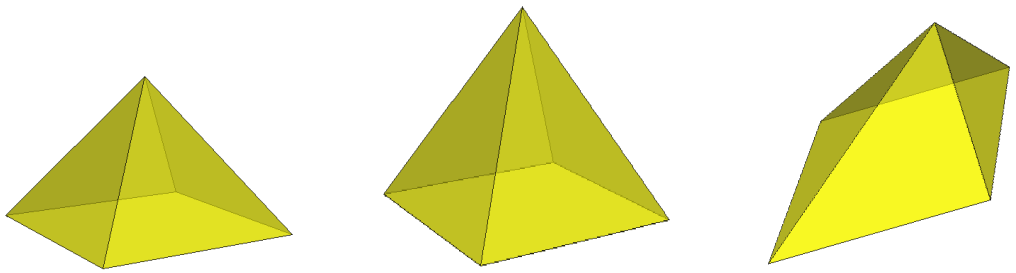

(a) (b) (c)

FIG. 12: (Color online) (a) A square pyramid with $\ell = \sqrt{2}h$. (b) A stretched square pyramid with $\ell < \sqrt{2}h$. (c) A sheared pyramid with a rhombic basal plane.

Consider a square pyramid with height h and length ℓ of the basal square (see Fig. 12). According to Proposition 2, the square pyramid lacks central symmetry and dense packings of this shape should be lattice packings of a centrally symmetric compound object made of the pyramids. We first consider the case when $\ell = \sqrt{2}h$, so that a pair of the pyramids that form a perfect contact through the square faces correspond to the regular octahedron (see Fig. 13a). Therefore, a dense packing of this special pyramid can be immediately obtained, which is exactly the densest lattice packing of octahedra with density $\phi = 18/19 = 0.974368\ldots$.

For the square pyramid with $\ell \neq \sqrt{2}h$, a centrally symmetric compound dimer can still be constructed in a similar way, which corresponds to a octahedron that is stretched ($\ell < \sqrt{2}h$) or compressed ($\ell > \sqrt{2}h$) along the direction of the height of the pyramids. To obtain dense packings of such pyramids, one can apply an affine transformation to the densest lattice packing of regular octahedron along one of its principal directions (see Fig. 13b), which leaves the packing density unchanged. This leads to a dense packing of stretched

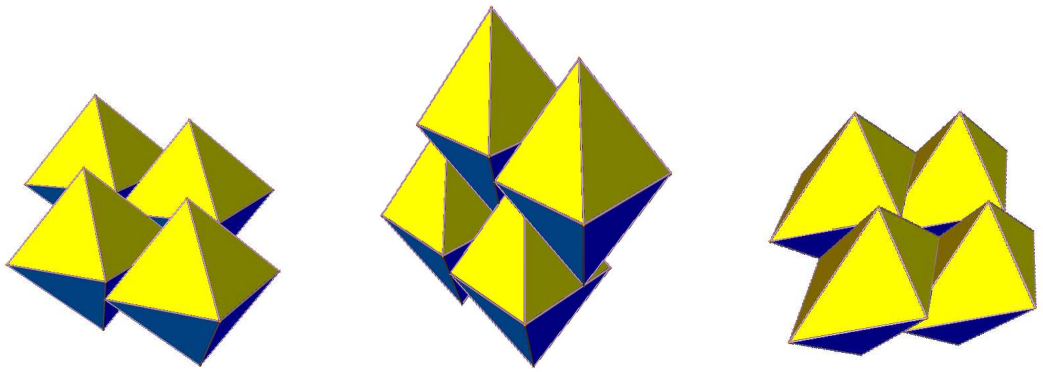

(a) (b) (c)

FIG. 13: (Color online) (a) A portion of a dense periodic packing of the square pyramids with $\ell = \sqrt{2}h$, whose fundamental cell contains two pyramid forming a centrally symmetric octahedra. (b) A portion of a dense periodic packing of the stretched square pyramids with $\ell < \sqrt{2}h$, which corresponds to an affine transformation of the densest packing of octahedra. (c) A portion of a dense periodic packing of the sheared pyramids, which corresponds to a sheared packing of octahedra.

(compressed) square pyramids with $\phi = 18/19 = 0.974368\ldots$ Similarly, for pyramids whose basal plane is a rhombus obtained by uniformly shearing the square, one can construct a dense packing of such objects by uniformly shearing the densest regular octahedron packing in the plane defined by a pair of the principal directions of an octahedra, resulting in the same density (see Fig. 13c).

We note that the constructed packings of the various aforementioned pyramids may not correspond to their associated densest packings, but these constructions should be close to the optimal ones. Once a construction is obtained by applying the organizing principles, one can perform various types of optimizations to improve the density by finding the (locally) densest configuration [45].

D. Equilibrium High-Density Crystal Phases

At infinite pressure, the optimal (densest) packing of hard particles corresponds to the thermodynamic equilibrium phase for these particles. In the case of identical hard spheres, the face-centered-cubic lattice is the thermodynamically favored maximal density state; see Fig. 2. Colloidal particles can synthesized to interact with effective hard-particle potentials

[9], and thus, it is useful to see to what extent the solid phase associated with the densest packing structure is stable under finite pressure by decompressing the packing using computer simulations [70]. Therefore, our general organizing principles enable one to obtain the equilibrium crystalline phase behavior of the hard particles at high densities. To illustrate this application, we consider the decompression of the densest known packing of truncated tetrahedra.

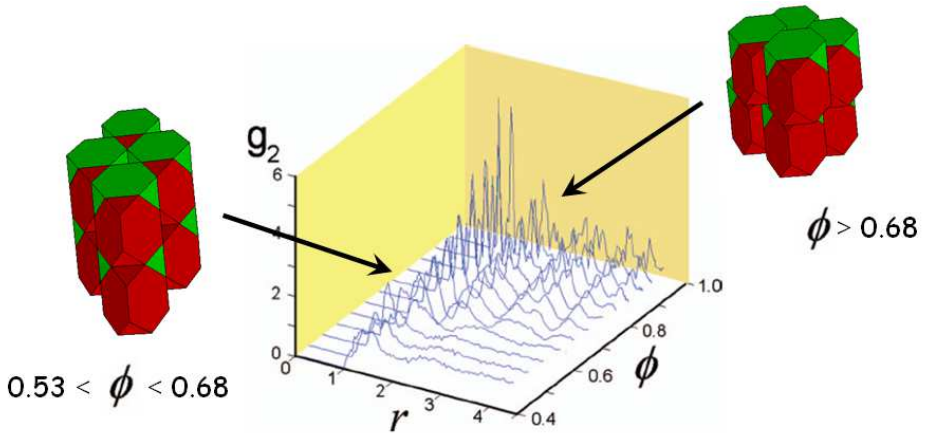

FIG. 14: (Color online) Pair correlation function $g_2(r)$ associated with the centroids of the truncated tetrahedra at different densities in the range from 0.99 to 0.38 during the melting of the highest-packing-fraction crystal [49]. Our simulation suggests that the melting process has two stages, including a solid-solid transition at a high density and a solid-liquid transition at an intermediate density [49]. At very high densities, $g_2(r)$ is a long-ranged function and the stable phase is associated with the densest packing of truncated tetrahedra. At intermediate densities, the stable phase is associated with a less dense packing of truncated tetrahedra with higher symmetry. Below $\phi \approx 0.53$, $g_2(r)$ suddenly changes from a long-ranged function to an exponential decaying function, indicating the occurrence of a first-order crystal-liquid transition.

For truncated tetrahedra, Monte-Carlo (MC) simulations have been carried out [49] to "melt" the densest known packing structure via a decompression process. In particular, a periodic simulation box containing $N = 686$ particles is employed, whose size and shape are allowed to change [41, 42]. The volume of the simulation box is slowly increased to decrease the pressure and density (i.e., packing fraction) of the system. At each density, a total number of 10 million MC trial moves are applied to each particle and 100 000 trial volume-preserving deformations are applied to the simulation box to equilibrate the

systems. Equilibrium structural characteristics, such as the pair-correlation function g_2 (see Fig. 14) and the number of dimers n_2 of truncated tetrahedra, are collected. Such descriptors are used to gauge the remaining crystalline order in the system during the decompression process. It is found that above $\phi \approx 0.68$, the crystal configurations associated with the optimal packing of truncated tetrahedra is the stable solid phase for these particles. When $0.53 < \phi < 0.68$, the crystal configurations associated with a packing with lower density but higher symmetry [49] becomes the stable phase. This suggests that the melting process has two stages, including a solid-solid transition a high density and a solid-liquid transition at an intermediate density [49]. Whether the crystalline phases are indeed the ones that we have identified via the decompression process must still be verified using other techniques [71]. Below $\phi \approx 0.53$, the correlation function g_2 suddenly changes from a long-ranged function to an exponential decaying function (see Fig. 14) and n_2 quickly drops from $N/2$ to almost zero, indicating the occurrence of a first-order crystal-liquid transition.

The wide range of stability for the crystal phases [$\phi \in (0.53, 0.995)$] is due to the fact that the dimers of truncated tetrahedra can fill space very efficiently, as can be seen from the amazingly high packing density (i.e., $207/208 = 0.995\ldots$; see Table I). This means that the free volume associated with crystals of the truncated tetrahedra is readily maximized in the dimer arrangement, leading to a lower free energy of the system. Since a dimer is formed by a pair of truncated tetrahedra contacting through the a common large hexagonal face, it is relative easy for such local clusters to form in a relatively dense liquid. Once such dimers nucleate, the system is expected to crystallize easily upon further compression. We note that the aforementioned decompression simulations can only provide estimates of the phase transition densities, the exact coexistence range of ϕ and whether there are higher-order solid-solid phase transitions can be precisely explored by carrying out free-energy calculations.

Similar complex high-density phase behaviors have also been observed in other nonspherical-hard-particle systems. For example, for ellipsoids with revolution at intermediate and large aspect ratios, it has been shown from decompression simulations [67], free-energy calculations [68] and replica exchange Monte Carlo simulations [69] that the densest known 2-particle basis packings constructed by Donev et al. [35] correspond to the stable high-density equilibrium phases. As the density decreases, nematic phases becomes the stable phases and the system undergoes a solid-liquid-crystal phase transition [67, 69].

For cube-like superballs, decompressing the densest known crystalline packings via molecular dynamics reveals the stability of the crystal phases associated with these packings and a solid-liquid-crystal transition to cubatic phases [65]. More recent free-energy calculations [38] also showed that the densest known packings of superballs correspond to the high-density equilibrium phases, while at intermediate densities, instead of cubatic phases, the FCC-plastic-crystal phases are stable.

The aforementioned complex melting processes associated with nonspherical particles are much richer than for hard-sphere system in which there is one type of crystal all the way down from the densest packing to the melting point. Because the rotational degrees of freedom and symmetries of a hard nonspherical particle can result in a variety of different high-density phases (as opposed to the simple case of identical spheres) [49, 53, 65, 66, 69], one must be careful to extend our conjectures and propositions that apply to high densities to predict equilibrium phases at intermediate densities (e.g., liquid-solid transitions).

V. CONCLUSIONS AND DISCUSSION

In this paper, we have provided general organizing principles for maximally dense packings of nonspherical hard particles, based on the most comprehensive set of packings of both convex and concave particles to date. For polyhedron particles, a general rule for achieving high packing densities is form a large number of face-to-face contacts, allowing particle centroids to be closer to one another. Therefore, despite whether the particle is convex or concave, central symmetry plays an important role in determining the dense packing structures. For centrally symmetric (convex or concave) particles, the densities of their densest Bravais-lattice packings provide tight lower bounds on the corresponding maximal packing densities that, according to Propositions 1 and 3, could be the optimal ones. This is due to the fact that when all the particles are aligned in the same direction, the central symmetry of the particle allows a large number of face-to-face contacts. For particles lacking central symmetry, their densest lattice packing contains a large number of vertex-to-face contacts which always leads to a low packing density. Instead, the densest lattice packing of a centrally symmetric compound unit of the original particles (i.e., a periodic packing of the original particles) provides a tight lower bound on the maximal packing density that, according to Propositions 2 and 4, could be the optimal one.

Organizing principles for certain smoothly-shaped particles, such as ellipsoids and superballs, have also been provided. A major difference between such smooth particles and a polyhedron is that the former possesses nontrivial surface curvature. A rule to obtain dense packings of particles with smooth surfaces, similar to that for polyhedra, is that the particles form contacts at surface regions with small local principal curvature (i.e., relatively "flat" regions). Thus, for centrally symmetric superballs, both numerical simulations and theoretical analysis suggest that the densest lattice packing of these shapes would be optimal. However, central symmetry alone does not seem to be sufficient to ensure that the densest packing of smooth particles is given by the corresponding optimal lattice packing. For example, for ellipsoids, which do not possess equivalent principal axes, periodic packings are constructed that are evidently denser than the optimal lattice packings. It could be that the elongation of an ellipsoid results in the local principal curvature that allows the rotational degrees of freedom of the particles to be fully explored. As noted in Sec. III, the role of curvature in determining dense packings for smoothly-shaped particles is still not very well understood.

Moreover, we have shown how our generalized organizing principles can be applied to construct analytically the densest known packings of certain convex nonspherical particles (e.g., centrally symmetric spherocylinders and "lens-shaped", as well as non-centrally symmetric square pyramids and rhombic pyramids). We have also shown that these principles can be profitably applied to infer the high-density crystalline phases of hard convex and concave particles.

We emphasize that while the propositions that we have put forth concerning dense packings of congruent nonspherical packings in the present paper currently lack the rigor of strict mathematical proofs, we expect that they will either ultimately lead to strict proofs or at least provide crucial guidance in obtaining such proofs for some nonspherical shapes. For example, in Ref. [42], we provided what we believe to be the major elements of a proof of Conjecture 1.

Can general principles be established that can be used to categorize and characterize disordered jammed packings according to the particle shapes and symmetries? This is in general a notoriously difficult question to answer, since disordered packings are intrinsically nonequilibrium states and can possess a wide spectrum of densities and degrees of disorder [9, 16]. Nonetheless, certain universal global structural features have begun to emerge from recent studies of the maximally random jammed (MRJ) states (analogs of the MRJ

state for spheres depicted in Fig. 1) of a wide class of nonspherical particles, regardless of the particle shapes or relative sizes (see Table IV). It has been shown that the MRJ packings possess special particle number density or local volume fraction fluctuations [31, 32], implying "hyperuniformity" of the packings over the large-scale structure and leading to anomalous quasi-long-range (QLR) correlations. This "hyperuniformity" property can be experimentally measured using standard scattering techniques and is manifested as a linear small-wavenumber (i.e., small-k) behavior in the structure factor [72] or the power spectrum [73]. It has been argued that the hyperuniform QLR correlations in MRJ packings arise from the competition between the requirement of jamming and maximal disorder. Therefore, the hyperuniform QLR correlations should be expected for a wide class of MRJ packings.

TABLE IV: Characteristics of MRJ packings of hard particles with different shapes, including spheres [9], ellipsoids [20], superballs [22], superellipsoids [23] and the non-tiling Platonic solids [31].

Particle	Isostatic	Hyperuniform QLR	MRJ Packing Fraction
Sphere	Yes	Yes	0.642
Ellipsoid	No (hypostatic)	Yes	$0.642 - 0.720$
Superball	No (hypostatic)	Yes	$0.642 - 0.674$
Superellipsoid	No (hypostatic)	Yes	$0.642 - 0.758$
Octahedron	Yes	Yes	0.697
Icosahedron	Yes	Yes	0.707
Dodecahedron	Yes	Yes	0.716
Tetrahedron	Yes	Yes	0.763

In addition, recent studies of MRJ packings of polyhedra [28, 30, 31] suggest that the isocounting conjecture proposed for sphere packings (i.e., each particle in the packing possesses $2n_{dof}$ constraints, where n_{dof} is the number of degrees of freedom) is also true for polyhedra (see Table IV). We note that for polyhedra, the number of constraints at each contact can be exactly given [28, 30, 31]. On the other hand, for smoothly-shaped particles, it was found that the MRJ packings are generally hypostatic, with each particle possessing a smaller number of contacts than $2n_{dof}$ [20–23, 25]; see Table IV. Moreover, it was shown that the surface curvature at contact points play an important role in blocking the rotation of the

particles and thus, in jamming the packing. However, it is difficult to quantify the effective number of constraints provided by each contact with different local principal curvatures. A successful quantification of this effective counting of constraints could lead to the conclusion that the iso-counting conjecture also holds for smoothly-shaped nonspherical particles.

Finally, we note that tunability capability via particle shape provides a means to design novel crystal, liquid and glassy states of matter that are much richer than can be achieved with spheres [9, 55]. For example, by introducing particle asphericity, a variety of optimal crystalline packings [35–52], diverse disordered jammed packings [20–32] as well as a wide spectrum of equilibrium phases [49, 53, 65–69, 74] have been obtained from computer simulations. On the experimental side, it has been recently shown [54] that silver polyhedral nanoparticles (with central symmetry) can self assemble into our conjectured densest lattice packings of such shapes [41, 42]. The resulting large-scale crystalline packings may facilitate the design and fabrication of novel three-dimensional materials for sensing [75], nanophotonics [76] and photocatalysis [77]. Our general organizing principles can clearly provide valuable guidance for novel materials design, which we will systematically investigate in future work. It will also be very useful to determine order maps for packings of nonspherical particles that are the analogs of Fig. 1 for sphere packings.

Acknowledgments

We are very grateful to Marjolein Dijkstra for giving us permission to adapt the figures of the octapod and tetrapod that appeared in Ref. [52]. This work was supported by the MRSEC Program of the National Science Foundation under Award Number DMR-0820341.

[1] J. D. Bernal, In *Liquids: Structure, Properties, Solid Interactions*. Hughel, T. J., Ed. (Elsevier, New York, 1965) pp. 25-50.

[2] R. Zallen, *The Physics of Amorphous Solids* (Wiley, New York, 1983).

[3] P. M. Chaikin and T. C. Lubensky, *Principles of Condensed Matter Physics* (Cambridge UP, New York, 2000).

[4] S. F. Edwards, *Granular Matter*, edited by A. Mehta (Springer-Verlag, New York, 1994).

[5] S. Torquato, *Random Heterogeneous Materials: Microstructure and Macroscopic Properties* (Springer-Verlag, New York, 2002).

[6] Liang, J. and Dill, K. A., Biophys J. **81**, 751 (2001).

[7] P. K. Purohit, J. Kondev, and R. Phillips, Proc. Natl. Acad. Sci. **100**, 3173 (2003).

[8] D. Ma, et al. Proc. Natl. Acad. Sci. **105**, 18800 (2008).

[9] S. Torquato and F. H. Stillinger, Rev. Mod. Phys. **82**, 2633 (2010).

[10] J. H. Conway and N. J. A. Sloane, *Sphere Packings, Lattices and Groups* (Springer, 1998).

[11] H. Cohn and N. Elkies, Ann. Math. **157**, 689 (2003).

[12] T. C. Hales, Annals of Mathematics **162**, 1065 (2005).

[13] K. Bezdek, *Classical Topics in Discrete Geometry* (Springer-Verlag, New york, 2010).

[14] G. Parisi and F. Zamponi, Rev. Mod. Phys. **82**, 789 (2010).

[15] S. Torquato, T. M. Truskett, and P. G. Debenedetti, Phys. Rev. Lett. **84**, 2064 (2000).

[16] Y. Jiao, F. H. Stillinger and S. Torquato, J. Appl. Phys. **109**, 013508 (2011).

[17] S. Torquato and F.H. Stillinger, J. Phys. Chem. B **105**, 11859 (2001).

[18] S. Torquato and F.H. Stillinger, J. Appl. Phys. **102**, 093511 (2007).

[19] This two-parameter description is but a very small subset of the relevant parameters that are necessary to fully characterize a configuration, but it nonetheless enables one to draw important conclusions [9]. For example, another axes that could be included is the mean contact number per particle, Z.

[20] A. Donev, *et. al.* Science **303**, 990 (2004).

[21] M. Mailman, C. F. Schreck, B. Chakraborty, and C. S. O'Hern, Phys. Rev. Lett. **102** 255501 (2009).

[22] Y. Jiao, F. H. Stillinger, and S. Torquato, Phys. Rev. E **81**, 041304 (2010).

[23] G.W. Delaney and P.W. Cleary, EPL **89**, 34002 (2010).

[24] S. Li, J. Zhao and X. Zhou, Chinese Phys. Lett. **25**, 4034 (2008).

[25] J. Zhao, S. Li, R. Zou and A. Yu, Soft Matter **8**, 1003 (2012).

[26] T. Li, S. Li, J. Zhao, P. Liu and L. Meng, Particuology **10**, 97 (2012).

[27] J. Baker and A. Kudrolli, Phys. Rev. E **82**, 061304 (2010).

[28] A. Jaoshvili, A Esakia, M. Porrati and P.M. Chaikin, Phys. Rev. Lett. **104**, 185501 (2010).

[29] K. C. Smith, M. Alam and T. Fisher, Phys. Rev. E **82**, 051304 (2010).

[30] K. C. Smith, T. Fisher and M. Alam, Phys. Rev. E **84**, 030301(R) (2011).

[31] Y. Jiao and S. Torquato, Phys. Rev. E **84**, 041309 (2011).

[32] C. Zachary, Y. Jiao and S. Torquato, Phys. Rev. Lett. **106**, 178001 (2011); C. Zachary, Y. Jiao and S. Torquato, Phys. Rev. E **83**, 051308 (2011); *ibid* 051309 (2011).

[33] A. Bezdek and W. Kuperberg, Applied Geometry and Discrete Mathematics: DIMACS Series in Discrete Mathematics and Theoretical Computer Science 4, edited by P. Gritzmann and B. Sturmfels (American Mathematics Society, Providence, RI, 1991), pp. 71 - 80

[34] J. M. Wills, Mathematika **38**, 318 (1991).

[35] A. Donev, F. H. Stillinger, P. M. Chaikin and S. Torquato, Phys. Rev. Lett. **92** 255506 (2004).

[36] Y. Jiao, F. H. Stillinger and S. Torquato, Phys. Rev. Lett. **100**, 245504 (2008).

[37] Y. Jiao, F. H. Stillinger and S. Torquato, Phys. Rev. E **79**, 041108 (2009)

[38] R. Ni, *et. al.* arXiv:1111.4357 (2011).

[39] U. Betke and M. Henk, Comput. Geom. **16**, 157 (2000).

[40] J. H. Conway and S. Torquato, Proc. Natl. Acad. Sci. **103**, 10612 (2006).

[41] S. Torquato and Y. Jiao, Nature **460**, 876 (2009)

[42] S. Torquato and Y. Jiao, Phys. Rev. E **80**, 041104 (2009).

[43] A. Haji-Akbari, *et. al.* Nature **462**, 773 (2009).

[44] Y. Kallus, V. Elser, and S. Gravel, Discrete Comput. Geom. **44**, 245 (2010).

[45] S. Torquato and Y. Jiao, Phys. Rev. E **81** 041310 (2010).

[46] E. R. Chen, M. Engel, and S. C. Glotzer, Discrete Comput. Geom. **44**, 253 (2010).

[47] Y. Kallus and V. Elser, Phys. Rev. E **83**, 036703 (2011).

[48] J. H. Conway, Y. Jiao and S. Torquato, PNAS **108**, 11009 (2011).

[49] Y. Jiao and S. Torquato, J. Chem. Phys. **135**, 151101 (2011).

[50] P. Damasceno, M. Engel and S. Glotzer, ACS Nano **6**, 609 (2012).

[51] L. Filion et al., Phys. Rev. Lett. **103**, 188302 (2009).

[52] J. de Graaf, R. van Roij, and M. Dijkstra, Phys. Rev. Lett. **107**, 155501 (2011).

[53] U. Agarwal and F. A. Escobedo, Nat. Mater. **10**, 230 (2011).

[54] J. Henzie, *et. al.* Nat. Mater. **11**, 131 (2012)

[55] S. Torquato, Invited talk at 2012 APS March Meeting (Abstract L33.00001). See also the following link for the presentation slides:
(http://absuploads.aps.org/presentation.cfm?pid=10202).

[56] M. D. Rintoul and S. Torquato, Phys. Rev. Lett. **77**, 4198 (1996); M. D. Rintoul and S.

Torquato, J. Chem. Phys. **105**, 9258 (1996).

[57] L. Fejes-Tóth, *Regular Figures* (Macmillan, New York, 1964).

[58] G. Kuperberg and W. Kuperberg, Discrete Comput. Geom. **5**, 389 (1990).

[59] J. Panos and P. K. Agarwal, *Combinatorial Geometry* (Wiley, New York, 1995).

[60] It is shown in Ref. [58] that for any convex shape in two-dimensions, the maximal packing density is bounded from below by $\sqrt{3}/2 = 0.866025\ldots$.

[61] S. Gravel, V. Elser and Y. Kallus, Discrete Comput. Geom. **46**, 799 (2011).

[62] This lattice packing corresponds to stacking layers of aligned cylinders such as the semisphere caps are packed as spheres in the face-centered cubic lattice.

[63] L. Fejes-Tóth, Discrete Comput. Geom. **1**, 307 (1986).

[64] A. Bezdek, W. Kuperberg and E. Makai, Discrete Comput. Geom. **6**, 277 (1991).

[65] R. D. Batten, F. H. Stillinger and S. Torquato, Phys. Rev. E **81**, 061105 (2010).

[66] A. Haji-Akbari, M. Engel and S. C. Glotzer, J. Chem. Phys. **135**, 194101 (2011).

[67] A. Donev, S. Torquato, and F. H. Stillinger, J. Comput. Phys. **202**, 765 (2005).

[68] M. Radu, P. Pfleiderer, and T. Schilling, J. Chem. Phys. **131**, 164513 (2009).

[69] G. Odriozola, J. Chem. Phys. **136**, 134505 (2012).

[70] D. Frenkel and B. Smit, *Understanding Molecular Simulation: From Algorithms to Applications.* (Academic Press, 2002).

[71] In future work, we will slowly compress dense liquid states of truncated tetrahedra to examine whether the resulting crystalline phases are the same as the ones that we identified via decompression of the putative densest packing of this Archimedean solid [49]. Precise free energy computations will provide of course the best way to ascertain the phase behavior of truncated tetrahedra over the allowable range of densities.

[72] S. Torquato and F. H. Stillinger, Phys. Rev. E **68**, 041113 (2003).

[73] C. E. Zachary and S. Torquato, J. Stat. Mech.: Theory and Experiment, P12015 (2009).

[74] P. F. Damasceno, M. Engel and S. Glotzer, arXiv.1202.2177 (2012).

[75] A. V. Kabashin, et al. Nature Mater. **8**, 867 (2009).

[76] C. Novo, A. M. Funston, and P. Mulvaney, Nature Nanotech. **3**, 598 (2008).

[77] W. H. Hung, et al., Nano Lett. **10**, 1314 (2010).